



Application of Taguchi-Based GRA Approach for Predictive Modelling of Perovskite Solar Cell

Nabilah Ahmad Jalaludin¹, Khairul Imran Kasirul Kasinathan¹, Fauziyah Salehuddin^{1,*}, Khairil Ezwan Kaharudin^{1,2}, Faiz Arith¹, Anis Suhaila Mohd Zain¹, Ibrahim Ahmad³, Siti Aisah Mat Junos¹, Prakash R. Apte⁴

¹ Micro & Nano Electronics (MiNE), CeTRI, Faculty of Electronics & Computer Technology and Engineering (FTKEK), Universiti Teknikal Malaysia, Hang Tuah Jaya, 76100 Durian Tunggal, Melaka, Malaysia

² Faculty of Engineering, Lincoln University College (Main Campus), Wisma Lincoln, 47301 Petaling Jaya, Selangor, Malaysia

³ College of Engineering (CoE), Universiti Tenaga Nasional (UNITEN), 43009 Kajang, Selangor, Malaysia

⁴ Indian Institute of Technology (IIT), Bombay, Powai, Mumbai 400076, India

ABSTRACT

The aim of this research is to optimize the perovskite cell (PSC) device using the Taguchi-based GRA method. In order to conduct this study, the simulation of perovskite cell device was carried out using the solar cell capacitance simulator (SCAPS-1D). Predictive modelling was further conducted to optimize multiple output responses such as power conversion efficiency (PCE), fill factor (FF), open circuit voltage (Voc) and short circuit current (Jsc). The optimization is finalized by determining the best combination of control factors and experiments to achieve maximum efficiency. This research methodology consists of three phases starting with the determination of PSC structure and electrical parameters, followed by numerical modelling using SCAPS-1D and predictive modelling using Taguchi-based GRA approach in optimizing the design. Next in phase 3, verification and benchmarking of output parameter results for mixed halide PSC with the experimental results from previous studies have been obtained. The studied design has achieved an efficiency of 25.27%, 83.34% fill factor, 1.24V open circuit voltage and 24.45 mA/cm² of short circuit current. Finally, the conducted research has achieved the objective of optimizing the PSC in improving the efficiency of the device.

Keywords:

Mixed halide; PCE; Photovoltaic; Taguchi based GRA

1. Introduction

Mixed halide perovskite solar cell research has increased significantly over the past several years, mostly because of its outstanding power conversion efficiency, ease of processing and reduced weight, all of which are essential for the low-cost thin-film photovoltaic sector. The existing silicon-based solar cells can be replaced with the mixed halide perovskite technology due to its simplicity of production, low cost, and quick energy payback [1]. In 2009, the first recorded photovoltaic cell using

* Corresponding author.

E-mail address: fauziyah@utem.edu.my

<https://doi.org/10.37934/araset.59.2.99109>

perovskite ($\text{CH}_3\text{NH}_3\text{PbI}_3$) had an efficiency of 3.81%; however, recently, this PCE has grown dramatically and is now above 20%.

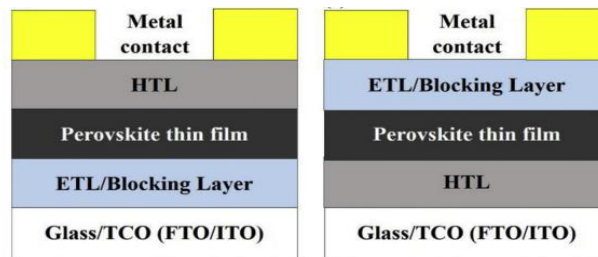
The perovskite structures most commonly studied exhibit elevated carrier recombination, weak carrier transport, and unfavourable defect densities. These issues have to be solved by investigating the effects of control factors on the performance and efficiency of PSC device. Interfaces within mixed halide perovskite cells, such as the perovskite/electron transport layer or perovskite/hole transport layer interfaces, play a critical role in device performance [2]. The problem statement could involve improving the interface engineering techniques to enhance charge transport, reduce recombination losses and optimize device performance. Various perovskite cell devices are found to have low efficiency after they have been fabricated. While mixed halide perovskite cells have shown impressive power conversion efficiencies, there is always room for improvement [3]. The purpose is always the aim to enhance the efficiency, performance and power output of the cells by optimizing the material composition, device architecture or fabrication processes. Numerical and predictive modelling along with Taguchi-based GRA method will be performed in order to analyse and optimize the PSC device [4].

The two mixed halide perovskites that are most frequently applied in photovoltaic cells are $\text{CH}_3\text{NH}_3\text{PbI}_{3-x}\text{Cl}_x$ and $\text{CH}_3\text{NH}_3\text{PbI}_{3-x}\text{Br}_x$, which have a number of benefits including improved carrier transport, reduced carrier recombination, increased carrier diffusion length, increased device stability and wideband optical absorptions [5]. The absorber layer of $\text{CH}_3\text{NH}_3\text{PbI}_{3-x}\text{Cl}_x$ for perovskite-based structures is frequently placed next to electron transport layer (ETL) and hole transport layer (HTL). The act of absorbing light occurs in which the input photon stimulates the electrons/holes that demonstrates the significance of the carrier passage from the absorber to the cathode and the anode which has a significant influence on perovskite-based devices [6,7].

The effective PCE of several mixed perovskites are such as those containing a combination of monovalent organic and/or inorganic cations and/or monovalent anions. In order to increase the efficiency and stability of solar systems that use these kinds of materials as an absorber layer, mixed halide perovskite materials have been created [2,3]. In PSC, an electron transport layer (ETL) and a hole transport layer (HTL) are sandwiched by a perovskite absorber layer that is a few hundred nanometres thick. This absorber layer might have a mesoporous scaffold or not. After light is absorbed, carriers like electrons and holes are generated. The result is that carriers move via a hauling channel while being stimulated by incident photon [8]. Along with the discussed topic, PSCs have emerged as one of the best cost-effective and efficient sources of green energy. Organolead mixed halide perovskite has the generic formula of $\text{ABX}_3\text{-Y}_x$, where A is a monovalent cation [A = methylammonium (MA), formamidinium (FA), and cesium (Cs)]; B is a divalent inorganic metal cation (Pb or Sn); X is a halide anion (Cl^- , Br^- , and I^-) while Y is another halide anion (Cl^- , Br^- , and I^-) [9]. Two major device architectures are documented for the PSCs; planar heterojunction (n-i-p) and inverted structure (p-i-n) are shown in Figure 1. For planar heterojunction PSCs, the ETL is coated on a glass substrate that contains transparent conducting oxide (TCO). After the ETL layer is covered with a perovskite film, the hole transport layer (HTL) is applied. For planar heterojunction PSCs, Spiro-OMeTAD as HTL and metal oxides (TiO_2 , ZnO , SnO_2) as ETL are often used. Finally, a carbon or metal (Ag, Au, or Mo) contact is deposited. In the case of inverted structured PSCs, the hole transport layer, perovskite film and ETL are deposited on the glass substrate used for TCO. Metal or carbon contact completes the circuit at the end [10].

The perovskite absorber contributes significantly to the device's performance. In this simulation conducted, the perovskite layer thickness is changed from 100 nm to 1000 nm. J_{SC} rises sharply with layer thickness up to 400 nm, and then rises very slowly after 500 nm. The substantial J_{SC} (24.59 mA/cm^2) obtained with a reasonable thickness of 400 nm is mostly caused by the perovskite's high

absorption coefficient. V_{OC} rises before 500 nm and then slightly declines after 500 nm, which is explained by the higher carrier recombination in the thicker absorber. With increasing perovskite thickness, the fill factor decreases monotonically, which is caused by rising series resistance. Additionally, the PCE first rises and reaches a maximum (20.96%) at 500 nm, then falls when absorber thickness is increased further [11-13].



(a) Planar heterojunction (b) Inverted structure
Fig. 1. Basic structure of Perovskite Cell

To attain high efficiency, the absorber layer's thickness is a crucial element. Within a specific level, the performance characteristics vary dramatically and as a result, increasing the absorber's thickness results in a reduction in efficiency. A successful collection of photo-generated carriers requires an absorber with a high enough absorber quality or carrier diffusion length. The thickness of the absorber layer is largely influenced by the solar cell's performance metrics. When layer thickness is low, the open-circuit voltage is large; as layer thickness rises, the voltage falls. After 700 nm of thickness, the V_{OC} is saturated. The highest value of the current density is 25.84 mA/cm^2 and it becomes saturated after reaching a value of roughly 25 mA/cm^2 . Due to a decrease in the electric field within the absorber, current density falls less with thicker absorbers. More recombination current will arise from an increase in absorber thickness if the quality of the absorber is inadequate [14].

Apart from the material thickness layer, the amount and characteristics of defects in the absorber layer could remarkably impact the performance of PSCs. It is found that a faulty state in the absorber layer would cause a considerable decline in device performance [15]. Device performance is essentially unaffected when the fault density in the perovskite layer is less than 10^{14} cm^{-3} . Device performance is significantly impacted when the defect density reaches 10^{14} cm^{-3} and declines sharply with increasing defect density. According to one research conducted previously, perovskite with a high crystallinity might reduce the defect densities [11]. This research investigates the effect of buffer and perovskite thickness and donor density as the control factor on the device performance based on vital parameters such as power conversion efficiency (PCE) and fill factor (FF).

For the best PSCs device performance, every device modelling must include optimization techniques. One of the key industrial processes to enhance product performance and reduce production costs is the optimization of manufacturing processes and products. Utilizing an optimization strategy for designing experiments based on Taguchi method is a methodical and effective way to do. In these situations, Taguchi method offer the most effective and practical answer with the fewest number of experimental trials [16-18]. This study was done by performing numerical simulation using SCAPS-1D software with the manipulation of control factors. The results were analysed using Taguchi method of L_9 orthogonal array alongside grey relational analysis (GRA) for a quicker optimization.

2. Methodology

2.1 Overall Project Method

The project methodology for this research consists of three phases as illustrated in Figure 2 which are defining the structure in phase 1 followed by numerical and predictive modelling in phase 2 and lastly, benchmarking the output values with previous journals.

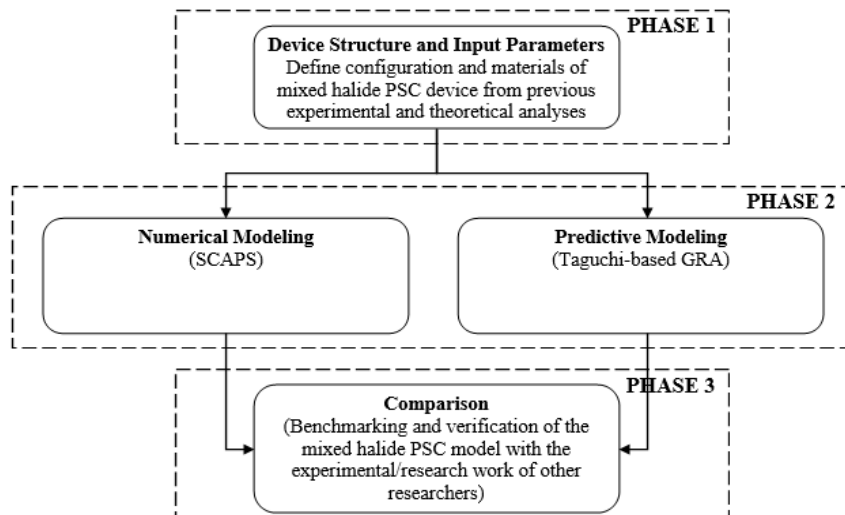


Fig. 2. Overall project flowchart

In phase 1, different ETLs, absorber thicknesses, and donor densities will be tested to find the best materials for maximizing cell performance. More simulations need to be conducted following the same approach with a variety of applied input parameters to find the best parameters for both materials. The key simulation parameters for the PSC device will be obtained from previous experimental and theoretical analyses.

After reviewing past researches that have been carried out, both numerical and predictive modelling of the PSC device should be ready to be performed. In phase 2 there are two types of modelling will be performed which are numerical modelling and predictive modelling. The main difference between these two modelling is that numerical modelling purely relies on numerical approach performed through software such as SCAPS-1D software whereas predictive modelling relies on the combination of both, numerical and predictive approaches such as statistic, machine learning and artificial intelligent [19,20].

In phase 3, for verification, the performance of the PSC device with the proposed parameters and the performance of the PSC device with different buffer and absorber thickness and donor density will be compared. The simulation results of PSC devices obtained from the proposed material was identified and compared with the experimental/research work of other researchers. It will also summarize the benchmark for this project.

2.2 Device Structure

The project methodology for this research consists of three phases as illustrated in Figure 2 which are defining the structure in phase 1 followed by numerical and predictive modelling in phase 2 and lastly, benchmarking the output values with previous journals.

The simulation cell designed shown in Figure 3, where fluorine-doped tin oxide ($\text{SnO}_2\text{:F}$) and spray-pyrolyzed zinc oxide (ZnO) were used as the n-type transparent conducting oxide (TCO) and buffer layer respectively. The device's front contact and rear contact, each had a metal work function set at 5.3931eV and 4.0204eV respectively. As the absorber layer, mixed halide perovskite ($\text{CH}_3\text{NH}_3\text{PbI}_{3-x}\text{Cl}_x$) was used to lightly capture electrons and holes. The charge extraction effectiveness and its stability in solar cell architecture has become the reason for the decision for Spiro-OMeTAD to be employed as hole transport material (HTM) in the configuration [21,22]. The aim of this work is to study the performance analysis by changing the buffer and absorber thickness and donor density.

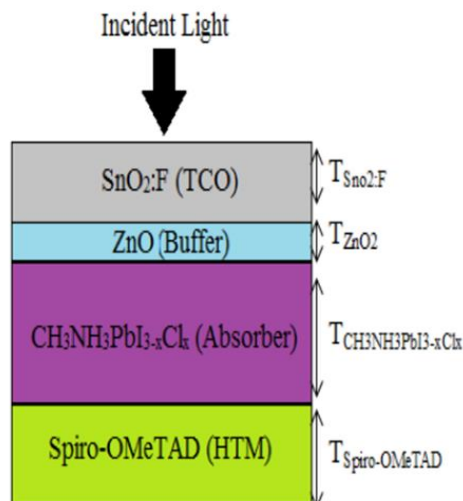


Fig. 3. PSC material design

Simulation parameters applied in this numerical modelling including the control factors applied in this research such as layer thickness and donor density are summarized in Table 1 [23]. The term χ , ϵ_r , E_g , μ_n , μ_p , N_v , N_c , N_a , N_d and N_t stands for electron affinity, relative permittivity, bandgap energy, electron mobility, hole mobility, effective valence band density, effective conduction band density, acceptor density, donor density and defect density respectively.

Table 1
 Baseline parameters for Perovskite Cell

Parameters	ETL	Buffer	Absorber	HTL
Thickness (μm)	0.2	0.04	0.4	0.25
χ (eV)	4	3.9	3.9	2.45
ϵ_r	9	9	6.5	3
E_g (eV)	3.5	3.3	1.55	3.0
μ_n (cm^2/Vs)	20	50	2	2×10^{-4}
μ_p (cm^2/Vs)	10	5	2	2×10^{-4}
N_v (cm^{-3})	1.8×10^{19}	1×10^{19}	1.8×10^{19}	1.8×10^{19}
N_c (cm^{-3})	2.2×10^{18}	1×10^{19}	2.2×10^{18}	2.2×10^{18}
N_a (cm^{-3})	-	-	-	2.0×10^{18}
N_d (cm^{-3})	1.0×10^{18}	5×10^{17}	1.0×10^{13}	-
N_t (cm^{-3})	10^{15}	10^{15}	2.5×10^{13}	10^{15}

Table 2 shows the defect interfaces for all the available interfaces. There are three interfaces in this design which are ETL/Buffer, Buffer/Absorber and Absorber/HTL. All these interface defects are kept constant based on the stated values for all interfaces.

Table 2
 Defect parameters for interfaces

Parameters	Defects
Defect Type	Neutral
Capture Cross Section Electrons (cm ²)	1.0 x 10 ⁻¹⁹
Capture Cross Section Holes (cm ²)	1.0 x 10 ⁻¹⁹
Energetic Distribution	Single
Reference for Defect Energy Level Et	Above the highest EV
Energy with Respect to Reference (eV)	0.600
Total Density (Integrated Over All Energies) (1/cm ²)	1.0 x 10 ¹⁰

Table 3 illustrates the control factors which are set to be varied throughout performing the Taguchi method optimization. There are four different control factors denoted as A, B, C and D which are varied. Each parameter consists of three levels. Each control factor is to be varied for every single experiment runs.

Table 3
 Level of control parameters

Symbol	Control Factor	Unit	Level		
			1	2	3
A	Buffer Thickness	μm	0.4	0.7	0.9
B	Buffer Donor Density	cm ⁻³	5×10 ¹⁷	5×10 ¹⁸	5×10 ¹⁹
C	Perovskite Thickness	μm	0.04	0.06	0.08
D	Perovskite Donor Density	cm ⁻³	1×10 ¹³	1×10 ¹⁴	1×10 ¹⁵

2.3 Taguchi Method

This project utilized the Taguchi method to determine the optimal solution for PSC devices. Taguchi method emphasizes the design and execution of experiments that can determine the effect of input process parameters on output responses. By analysing the impact of different components, the optimal combination of factors can be identified [20]. Figure 4 depicts the primary implementation processes for Taguchi method input process parameter optimization. The selection of the Orthogonal Array (OA) depended on the number of electrical parameters chosen. As the simulation is carried out for four different electrical parameters, hence L₉ OA was chosen to be employed as the optimization approach for this research.

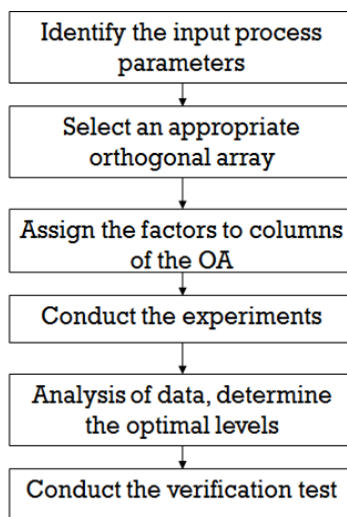


Fig. 4. Taguchi-based GRA method flowchart

3. Results and Discussion

3.1 SCAPS-1D Simulation

Figure 5 shows the current to voltage (I-V) plot obtained from the simulation conducted using SCAPS-1D software. This graph illustrates that voltage increases exponentially with current. In the context of this research output parameter, it means that the open circuit voltage has an exponential growth along with the short circuit current.

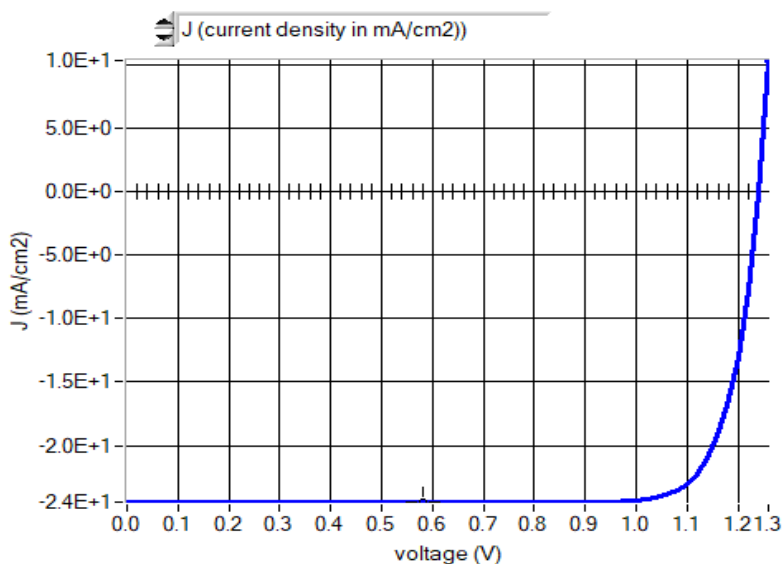


Fig. 5. I-V curve

3.2 Taguchi-Based GRA Analysis

Table 4 shows the output responses of fill factor (FF) and power conversion efficiency (PCE), open circuit voltage (V_{OC}) and short circuit current (J_{SC}) obtained for all nine experiment runs based on Taguchi method L_9 OA. Each of the output parameters taken upon conducting each combination of experiments based on the DoE. Although there is an increase in efficiency, however, this result is yet

to be optimized by further computing the grey relational coefficient (GRC) and grey relational grade (GRG).

Table 4
 Output optimization using Taguchi-based GRA method

Exp. No.	Control Factor				Measurements of Output			
	A	B	C	D	FF	PCE	V _{oc}	J _{sc}
1	1	1	1	1	21.62	1.27	83.64	23.01
2	1	2	2	2	23.58	1.25	83.36	24.64
3	1	3	3	3	24.45	1.24	83.34	25.27
4	2	1	2	3	23.58	1.25	83.53	24.67
5	2	2	3	1	24.45	1.24	82.96	25.15
6	2	3	1	2	21.62	1.27	83.93	23.06
7	3	1	3	2	24.45	1.24	82.94	25.14
8	3	2	1	3	21.62	1.27	83.99	23.06
9	3	3	2	1	23.58	1.25	83.37	24.64

The experimental results from the GRA in Table 5 reveals that the highest rank of GRG demonstrated by the third experimental row, indicating that the third row contains the best levels of the input material parameters which would possibly generate the most optimum magnitude for PCE of the device. It is observed that the maximum fitness value (GRG) is measured at 0.928439 in which the corresponding value of material parameter; buffer thickness, buffer donor density, perovskite thickness and perovskite donor density are predicted to be 0.7 μm (level 2), 5×10¹⁹ cm⁻³ (level 3), 0.8 μm (level 3) and 1 x 10¹⁵ cm⁻³ (level 3) respectively.

Table 5
 Computed GRC and GRG

Exp. No.	Grey Relational Coefficient				GRG
	J _{sc}	V _{oc}	FF	PCE	
1	0.3333	0.9084967	0.600575	0.333333	0.725246
2	0.6197	0.4729679	0.455338	0.640481	0.729482
3	0.9998	0.3398533	0.445629	1	0.928439
4	0.6196	0.4621352	0.534527	0.65343	0.756578
5	1	0.3380168	0.337097	0.902293	0.859128
6	0.3333	1	0.900862	0.338065	0.857423
7	1	0.3333333	0.333333	0.893386	0.853351
8	0.3334	0.9705198	1	0.339078	0.880984
9	0.6197	0.4776632	0.458333	0.644128	0.73326

The perovskite solar cell is then re-simulated using the predicted value of material parameters as shown in Table 6 for verification.

Table 6
 GRG of output parameters at different level

Symbol	Control Factor	GRG			Optimized Level	Overall Mean of GRG (γ _m)
		Level 1	Level 2	Level 3		
A	Buffer Thickness	0.7944	0.8244	0.8225	2	0.8138
B	Buffer Donor Density	0.7784	0.8232	0.8397	3	
C	Perovskite Thickness	0.8212	0.7398	0.8803	3	
D	Perovskite Donor Density	0.7725	0.8134	0.8553	3	

Table 7 illustrates the final optimization using Taguchi-based GRA method. It is verified that the results obtained through multiple optimizations using the Taguchi method and the optimization with the Taguchi-based GRA method yield the same optimal output parameters. It is observed that the PCE of the solar cell has been improved by ~23.2% after being optimized using the Taguchi-based GRA. On the other hands, the V_{OC} of the device suffers a marginal decline for ~2.4% after being optimized using the proposed predictive analytics. Nevertheless, both FF and J_{SC} exhibits an improvement by ~12.3% and ~11.6% respectively as shown in Table 7. Based on the comparative results, it is concluded that a Taguchi-based GRA approach can be regarded as a practical approach to optimize the material parameters of the perovskite solar cell in attaining better cell performances. This approach could also be suitably employed in modelling multiple material parameters of Perovskite photovoltaic cell for improved performance.

Table 7
 Final optimization comparison

Output Parameter	Before Optimize	After Optimization (Taguchi Method)		Optimize with Taguchi-GRA [my work]	Optimize with another approach [4]
		Individual	Multiple		
PCE (%)	19.41	25.27	25.27	25.27	20.6
FF (%)	73.11	83.93	83.34	83.34	77.72
V_{OC} (V)	1.27	1.27	1.24	1.24	1.134
J_{SC} (mA/cm ²)	21.62	24.45	24.45	24.45	21.47

4. Conclusions

Mixed halide perovskite cell is a perovskite solar cell which uses an absorber layer which consist of two types of halogen element. In traditional perovskite solar cells, the most commonly used halogen is iodine (I), resulting in a material known as methyl-ammonium lead iodide ($CH_3NH_3PbI_3$). However, by introducing additional halogen elements such as bromine (Br) or chlorine (Cl), mixed halide perovskites can be formed such as $CH_3NH_3PbI_{3-x}Cl_x$. Mixed halide perovskites offer other advantages like enhanced stability and reduced sensitivity to environmental factors. The incorporation of bromine or chlorine atoms can help improve the material's resistance to moisture, heat and other degradation causes. The simulation was implemented by employing a fully simulated mixed halide PSC device structure which composed of $SnO_2:F/ZnO/CH_3NH_3PbI_{3-x}Cl_x/Spiro-OMeTAD$. By employing SCAPS-1D software, the study can evaluate the feasibility of mixed halide perovskite cells and identify optimal halide compositions to achieve desired performance characteristics. The numerical simulations conducted with SCAPS-1D software enable a comprehensive analysis of the electrical and optical properties of the cells, aiding in the establishment of design guidelines and providing insights for future research directions.

After optimization using Taguchi method have been done, the parameter that have significant effect on the design is perovskite thickness. It is proven that the thickness of perovskite has massive impact on optimizing the efficiency of mixed halide perovskite device. By identifying the crucial control factor, it is possible to enhance charge carrier dynamics, reduce energy losses, improve light absorption and enhance charge transport carriers. By using the Taguchi-based GRA approach, the gained OA simulation results were analysed. The simulation results showed that mixed halide perovskite solar cell has produced an initial efficiency of 23.01% compared to previous researches using the similar cell configuration achieved an optimal PCE of 19.41% by undergoing numerical modelling through SCAPS-1D. Furthermore, after optimization using Taguchi-based GRA by utilizing the L_9 OA, the efficiency increased to 25.27%.

Acknowledgement

The authors would like to thank the Ministry of Higher Education (MOHE) for sponsoring this work under project (FRGS/1/2022/TK07/UTEM/02/47) and MiNE, CeTRI, Faculty of Electronics & Computer Technology and Engineering (FTKEK), Universiti Teknikal Malaysia Melaka (UTeM) for the moral support throughout the project. The authors would also like to thanks Dr. Marc Burgelman of the University of Gent in Belgium for supplying the SCAPS 1D simulation program.

References

- [1] Dubey, Ashish, Eman A. Gaml, Nirmal Adhikari, Khan Mamun Reza, H. Zeyada, and Qiquan Qiao. "Engineering of ambient processing conditions to control solvent induced intermediate phase in mixed halide organic-inorganic perovskite ($\text{CH}_3\text{NH}_3\text{PbI}_{3-x}\text{Cl}_x$) film for efficient planar perovskite solar cells." In *2016 IEEE International Conference on Electro Information Technology (EIT)*, pp. 0716-0722. IEEE, 2016.
- [2] Abena, AM Ntoug, A. Teyou Ngoupo, and J. M. B. Ndjaka. "Computational analysis of mixed cation mixed halide-based perovskite solar cell using SCAPS-1D software." *Heliyon* 8, no. 11 (2022). <https://doi.org/10.1016/j.heliyon.2022.e11428>
- [3] Murdey, Richard, Yasuhisa Ishikura, Yuko Matsushige, Shuaifeng Hu, Jorge Pascual, Minh Anh Truong, Tomoya Nakamura, and Atsushi Wakamiya. "Operational stability, low light performance, and long-lived transients in mixed-halide perovskite solar cells with a monolayer-based hole extraction layer." *Solar Energy Materials and Solar Cells* 245 (2022): 111885. <https://doi.org/10.1016/j.solmat.2022.111885>
- [4] Kaharudin, Khairil Ezwan, and Fauziah Salehuddin. "Predictive Modeling of Mixed Halide Perovskite Cell using Hybrid L27 OA Taguchi-based GA-MLR-GA Approach." *Jurnal Teknologi* 84, no. 1 (2022): 1-9. <https://doi.org/10.11113/jurnalteknologi.v84.15550>
- [5] Kakavelakis, George, Emmanouil Gagaoudakis, Konstantinos Petridis, Valia Petromichelaki, Vassilis Binas, George Kiriakidis, and Emmanuel Kymakis. "Solution processed $\text{CH}_3\text{NH}_3\text{PbI}_{3-x}\text{Cl}_x$ perovskite based self-powered ozone sensing element operated at room temperature." *Acs Sensors* 3, no. 1 (2018): 135-142. <https://doi.org/10.1021/acssensors.7b00761>
- [6] Widiyanto, Eri, Erlyta Septa Rosa, Kuwat Triyana, Natalita Maulani Nursam, and Iman Santoso. "Performance analysis of carbon-based perovskite solar cells by graphene oxide as hole transport layer: Experimental and numerical simulation." *Optical materials* 121 (2021): 111584. <https://doi.org/10.1016/j.optmat.2021.111584>
- [7] Chen, Jianhua, Yao Chen, Liang-Wen Feng, Chunling Gu, Guoping Li, Ning Su, Gang Wang *et al.*, "Hole (donor) and electron (acceptor) transporting organic semiconductors for bulk-heterojunction solar cells." *EnergyChem* 2, no. 5 (2020): 100042. <https://doi.org/10.1016/j.enchem.2020.100042>
- [8] Sobayel, K., Md Akhtaruzzaman, K. S. Rahman, M. T. Ferdaous, Zeyad A. Al-Mutairi, Hamad F. Alharbi, Nabeel H. Alharthi, Mohammad R. Karim, S. Hasmady, and N. Amin. "A comprehensive defect study of tungsten disulfide (WS_2) as electron transport layer in perovskite solar cells by numerical simulation." *Results in Physics* 12 (2019): 1097-1103. <https://doi.org/10.1016/j.rinp.2018.12.049>
- [9] Khan, Firoz, Mohd Taukeer Khan, Thamraa Alshahrani, Nafis Ahmad, A. M. Alshehri, Imran Fareed, Mustafa S. Elhassan, and Mohammad Shariq. "A comprehensive analysis of PV cell parameters with varying halides stoichiometry in mixed halide perovskite solar cells." *Optical Materials* 123 (2022): 111905. <https://doi.org/10.1016/j.optmat.2021.111905>
- [10] Nair, Saikumar, Siddhant B. Patel, and Jignasa V. Gohel. "Recent trends in efficiency-stability improvement in perovskite solar cells." *Materials Today Energy* 17 (2020): 100449. <https://doi.org/10.1016/j.mtener.2020.100449>
- [11] Lin, Lingyan, Linqin Jiang, Ping Li, Baodian Fan, and Yu Qiu. "A modeled perovskite solar cell structure with a Cu_2O hole-transporting layer enabling over 20% efficiency by low-cost low-temperature processing." *Journal of Physics and Chemistry of Solids* 124 (2019): 205-211. <https://doi.org/10.1016/j.jpcs.2018.09.024>
- [12] Bahrudin, Mohd Shaparuddin, Siti Fazlili Abdullah, Ibrahim Ahmad, Ahmad Wafi Mahmood Zuhdi, Azri Husni Hasani, Fazliyana Za'Abbar, Mazin Malik, and M. Najib Harif. "J sc and Voc Optimization of Perovskite Solar Cell with Interface Defect Layer Using Taguchi Method." In *2018 IEEE International Conference on Semiconductor Electronics (ICSE)*, pp. 192-196. IEEE, 2018.
- [13] Mandadapu, Usha, S. Victor Vedanayakam, K. Thyagarajan, and B. J. Babu. "Optimisation of high efficiency tin halide perovskite solar cells using SCAPS-1D." *International journal of simulation and process modelling* 13, no. 3 (2018): 221-227. <https://doi.org/10.1504/IJSPM.2018.093097>
- [14] Hossain, Md Faruk, Mohammad Faisal, and Hiroyuki Okada. "Device modeling and performance analysis of perovskite solar cells based on similarity with inorganic thin film solar cells structure." In *2016 2nd International*

- Conference on Electrical, Computer & Telecommunication Engineering (ICECTE)*, pp. 1-4. IEEE, 2016. <https://doi.org/10.1109/ICECTE.2016.7879585>
- [15] van Gorkom, Bas T., Tom PA van der Pol, Kunal Datta, Martijn M. Wienk, and René AJ Janssen. "Revealing defective interfaces in perovskite solar cells from highly sensitive sub-bandgap photocurrent spectroscopy using optical cavities." *Nature Communications* 13, no. 1 (2022): 349. <https://doi.org/10.1038/s41467-021-27560-6>
- [16] Mahbubah, N. A., M. Nuruddin, S. S. Dahda, D. Andesta, E. Ismiah, D. Widyaningrum, M. Z. Fathoni *et al.*, "Optimization of CNC turning parameters for cutting Al6061 to achieve good surface roughness based on Taguchi method." *Journal of Advanced Research in Applied Mechanics* 99, no. 1 (2022): 1-9.
- [17] Huan, Chow Yong, Wan Zuki Azman Wan Muhamad, Zainor Ridzuan Yahya, Nor Hizamiyani Abdul Azziz, Tan Li Mei, and Tan Xiao Jian. "Hybrid mahalnobis taguchi system with binary whale optimisation feature selection for the wisconsin breast cancer dataset." *Journal of Advanced Research in Applied Sciences and Engineering Technology* 31, no. 3 (2023): 93-105. <https://doi.org/10.37934/araset.31.3.93105>
- [18] Shakir, Safa Waleed, Sarah Saad Mohammed Jawad, and Zainab Abdulmaged Khalaf. "Analysis of the Impact of Nanofluids on the Improvement in CO2 Absorption using Taguchi Method." *Journal of Advanced Research in Fluid Mechanics and Thermal Sciences* 115, no. 1 (2024): 83-98. <https://doi.org/10.37934/arfmts.115.1.8398>
- [19] Abidin, Nurul Aliyah Zainal, Faiz Arith, Adri Aflah Shahrin Amri, Ahmad Nizamuddin Mustafa, Hafez Sarkawi, Mohd Shahadan Mohd Suan, Ahmad Syahiman Mohd Shah, Siti Aisah Junos, and Fauziyah Salehuddin. "Growth Time Dependence on ZnO Nanorods Photoanode for Solar Cell Applications." *Journal of Advanced Research in Applied Sciences and Engineering Technology* 31, no. 2 (2023): 339-351. <https://doi.org/10.37934/araset.31.2.339351>
- [20] Johari, Nur Aliesa, Nabilah Ahmad Jalaludin, Fauziyah Salehuddin, Faiz Arith, Khairil Ezwan Kaharudin, Anis Suhaila Mohd Zain, Siti Aisah Mat Junos, and Ibrahim Ahmad. "Analysis of Inverted Planar Perovskite Solar Cells with Graphene Oxide as HTL using L9 OA Taguchi Method." *Journal of Advanced Research in Micro and Nano Engineering* 16, no. 1 (2024): 48-60. <https://doi.org/10.37934/armne.16.1.4860>
- [21] Sabbah, Hussein, Jack Arayro, and Rabih Mezher. "Numerical simulation and optimization of highly stable and efficient lead-free perovskite FA1- xCsxSnI3-based solar cells using SCAPS." *Materials* 15, no. 14 (2022): 4761. <https://doi.org/10.3390/ma15144761>
- [22] Ritu, Gagandeep, Ramesh Kumar, and Fakir Chand. "Numerical simulation of a mixed-halide perovskite solar cell using doping gradient." *Journal of Computational Electronics* 22, no. 5 (2023): 1532-1540. <https://doi.org/10.1007/s10825-023-02085-x>
- [23] Widiyanto, Eri, Erlyta Septa Rosa, Kuwat Triyana, Natalita Maulani Nursam, and Iman Santoso. "Performance analysis of carbon-based perovskite solar cells by graphene oxide as hole transport layer: Experimental and numerical simulation." *Optical materials* 121 (2021): 111584. <https://doi.org/10.1016/j.optmat.2021.111584>